

# Embedding Graph Auto-Encoder with Joint Clustering via Adjacency Sharing

Xuelong Li<sup>1</sup> Hongyuan Zhang<sup>1</sup> Rui Zhang<sup>1</sup>

## Abstract

Graph convolution networks have attracted many attentions and several graph auto-encoder based clustering models are developed for attributed graph clustering. However, most existing approaches separate clustering and optimization of graph auto-encoder into two individual steps. In this paper, we propose a graph convolution network based clustering model, namely, Embedding Graph Auto-Encoder with JOint Clustering via Adjacency Sharing (*EGAE-JOCAS*). As for the embedded model, we develop a novel joint clustering method, which combines relaxed k-means and spectral clustering and is applicable for the learned embedding. The proposed joint clustering shares the same adjacency within graph convolution layers. Two parts are optimized simultaneously through performing SGD and taking close-form solutions alternatively to ensure a rapid convergence. Moreover, our model is free to incorporate any mechanisms (e.g., attention) into graph auto-encoder. Extensive experiments are conducted to prove the superiority of EGAE-JOCAS. Sufficient theoretical analyses are provided to support the results.

## 1. Introduction

Clustering, which plays import roles in plenty of applications, is one of the most fundamental topics in machine learning and pattern recognition. In past decades, a spectrum of algorithms have been proposed (Dunn, 1973; Ester et al., 1996; Nie et al., 2014). In particular, k-means (Dunn, 1973), which exploits density information to group samples, and spectral clustering (Shi & Malik, 2000; Ng et al., 2002), which aims to solve a graph cut problem, are two most popular methods. K-means assigns each sample to certain cluster and then updates all centroids of clusters according to current assignments. Spectral clustering constructs a similarity matrix (which can be regarded as a weighted graph) and then performs eigenvalue decomposition on its Laplacian matrix to obtain relaxed indicator matrix. Finally, group rows of indicator matrix through certain methods, such as k-means and spectral rotation. Drawbacks of these two algorithms are ob-

vious: K-means is too simple to work on non-spherical data while spectral clustering depends severely on construction of similarity.

With the rise of deep learning, many efforts have been made to promote capacities of traditional clustering models via neural networks (Shaham et al., 2018; Tian et al., 2014a). Auto-encoder (Hinton & Salakhutdinov, 2006) is a well-known deep model that can extract deep features by encoder and reconstruct raw features by decoder. Stacked Auto-Encoder (SAE) (Tian et al., 2014a) trains auto-encoder layer-wisely. An obvious drawback is that the clustering phase and auto-encoder training phase are independent. In other words, the extracted features may not be beneficial for clustering. DEC (Xie et al., 2016) embeds k-means with auto-encoders and optimizes both of neural network and k-means model by SGD. However, the optimization through SGD is inefficient since it needs lots of iterations to converge. Moreover, the relationship among data points may be neglected by auto-encoder as auto-encoder cannot process links between samples.

In recent years, graph convolution network (Scarselli et al., 2008; Wu et al., 2019) has attracted lots of attentions as it extends convolution operation and neural networks to graph type data. In network embedding, the goal is to learn representations for each node (or graph) (Wang et al., 2018). The learned embedding is used for graph classification, node clustering and link prediction. Similarly, graph auto-encoder (GAE) (Kipf & Welling, 2016) is an extension of auto-encoder, which learns node representation with adjacency and reconstructs the adjacency from the extracted features. The embedding is frequently used for node clustering and link prediction. However, it often suffers from overfitting and the generated representations may be unsuitable for clustering.

In this paper, we propose a graph auto-encoder based clustering model, Embedding Graph Auto-Encoder with JOint Clustering via Adjacency Sharing (*EGAE-JOCAS*). The main contributions include: **1)** EGAE-JOCAS incorporates a clustering model into graph encoder. Therefore, GAE and clustering model are optimized simultaneously, which can affect GAE to generate more appropriate representations for clustering. The optimization is composed of SGD and close-form solutions. **2)** We develop a novel clustering model,

named as joint clustering, to employ learned graph embedding more rationally. Joint clustering is a fusion of relaxed k-means and spectral clustering, and the adjacency is shared by both GAE and joint clustering. Meanwhile, we also design a decoder of GAE to generate adequate representations for joint clustering. **3)** EGAE-JOCAS can incorporate any more complicated mechanisms such as attention, pooling and so on.

**Notations:** In this paper, all matrices are represented by uppercase words and all vectors are denoted by bold lowercase words. For a matrix  $M$ ,  $\mathbf{m}^i$  is the  $i$ -th row vector,  $\mathbf{m}_j$  is the  $j$ -th column vector,  $\text{tr}(M)$  is the trace of  $M$ ,  $M^T$  is the transpose of  $M$  and  $M \geq 0$  means all elements are non-negative.  $I$  denotes the identify matrix,  $\mathbf{1}_n \in \mathbb{R}^n$  denotes vector whose elements are all 1.  $\nabla \cdot$  is the gradient operator.  $[x, \dots, y]$  and  $[x; \dots; y]$  denotes row and column vectors respectively.

## 2. Related Work

In this section, we first review works about graph convolution neural network for graph embedding. Then we introduce several representative models which aim to employ deep learning to perform clustering.

### 2.1. Graph Convolution Neural Network

Graph, which can describe complicated relationship, has been widely studied and applied in diverse applications, such as community network, bioscience, recommender system and so on (Bojchevski et al., 2018; Wang et al., 2017; Liu et al., 2015). GraphGAN (Wang et al., 2018) incorporates adversarial learning into graph embedding learning and develops a graph softmax function to utilize the structure of graph. Literature (Wang et al., 2017) combines graph embedding and clustering to perform clustering on graph. However, capacities of these methods are limited and they only utilize the shallow information of graph. As a result, they cannot make use of structure information effectively and exploit potential relationship among nodes.

Due to success of CNN, graph convolution neural networks have been studied widely in recent years. A focusing problem is how to extend convolution operation to irregular data. All existing convolution operations can be split as 2 categories, spectral based methods (Bruna et al., 2013; Kushnir et al., 2006; Kipf & Welling, 2017) and spatial based methods (Niepert et al., 2016; Micheli, 2009; Veličković et al., 2017) according to (Wu et al., 2019). On the one hand, spectral-based methods (Bruna et al., 2013; Kushnir et al., 2006; Kipf & Welling, 2017) are motivated by convolution theorem, the Fourier transformation and the characteristics of Laplacian operator (Shuman et al., 2013). In spectral-based models, the spectral domain is regarded as frequency

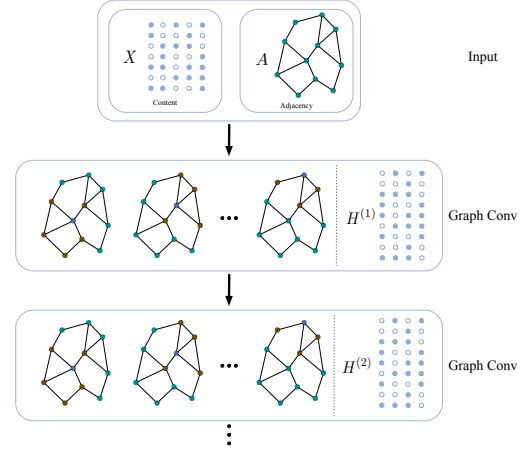


Figure 1. General graph convolution network architecture

domain which is a fundamental concept in the Fourier transformation. A natural thought is to use a normal matrix as convolutional kernel to learn. A distinct drawback is that parameters of kernels are too many to learn. To address this problem, (Bruna et al., 2013) assumes that the convolutional kernel in spectral domain is diagonal. To further reduce the amount of parameters to learn and promote efficiency of convolution, ChebNet (Kushnir et al., 2006) utilizes Chebyshev polynomials to approximate the convolutional kernel. On the other hand, spatial-based methods do not transform the domain and focus on how to select nodes to perform convolution. For example, PATCH-SAN (Niepert et al., 2016) orders other nodes for a node and chooses top  $k$  neighbors to perform convolution. In particular, GCN proposed in (Kipf & Welling, 2017) combines spectral-based models and spatial-based ones. It employs linear approximation of convolution kernels via Chebyshev polynomials. Moreover, it can be regarded as a spatial method which only considers 1-neighbor to perform convolution.

### 2.2. Deep clustering

Auto-encoder (Hinton & Salakhutdinov, 2006), as a classical variant of neural network for unsupervised learning, is often employed to perform clustering, such as SAE (Tian et al., 2014a) and StructAE (Peng et al., 2018). Roughly speaking, they employ a multi-layer neural network (encoder) to learn non-linear features and reconstruct raw features from the learned features by decoder. However, SAE and StructAE separate clustering from training auto-encoder. DEC (Xie et al., 2016) embeds k-means into auto-encoder but optimizes it by SGD. Actually, gradient descent is an approximate method when the objective function can not be solved directly. Therefore, SGD is not the best algorithm to solve embedding models such that DEC converges slowly. SpectralNet (Shaham et al., 2018), which is not based on auto-encoder, intends to perform spectral clustering with

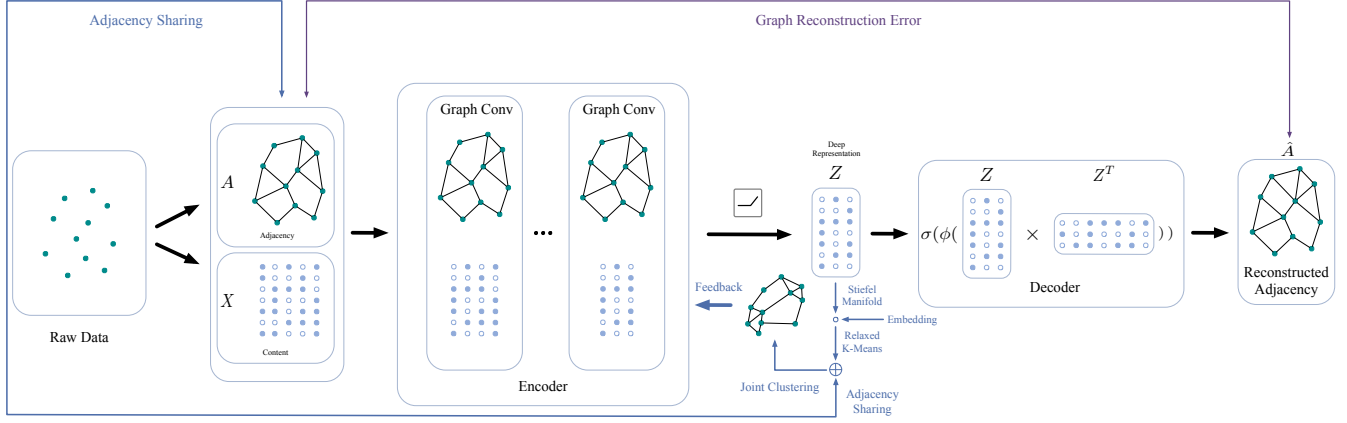


Figure 2. Conceptual illustration of EGAE-JOCAS. Inputs of EGAE-JOCAS consists of two parts, adjacency  $A$  and content  $X$ . After encoding, data is mapped into a latent feature space. Note that the last layer of encoder utilizes ReLU as activation function to ensure inner-products between any two points non-negative. Joint clustering is embedded into GAE to induce it to generate preferable embeddings.  $\hat{A}$  is the reconstructed adjacency and should be close to  $A$ . Note that any complicated layers (e.g., attention) can be integrated.

neural networks.

However, all these methods fail to utilize structure information provided by graph type data. Graph auto-encoder (Kipf & Welling, 2016; Pan et al., 2018) extends classical auto-encoder to graph but it fails to consider clustering. In this paper, we propose a novel model that embeds a joint clustering model into graph auto-encoder, so that it can exploit relationship of structure information.

### 3. Embedding Graph Auto-Encoder with Joint Clustering via Adjacency Sharing

In this section, we will show how the graph auto-encoder (GAE) works and propose the Embedding Graph Auto-Encoder with JOint Clustering via Adjacency Sharing (EGAE-JOCAS). In section 5, we will demonstrate the rationality of utilization of GAE from both intuitive aspect and theoretical aspect.

#### 3.1. Convolution on Graph

To apply convolution operation on irregular data, we utilize a graph convolution operation that can be explained as both spectral operator and spatial operator. According to the convolution theorem, the convolution operator can be defined from the frequency domain, which is conventionally named as spectral domain of graph signals. Formally, a spatial signal of graph  $x \in \mathbb{R}^n$  can be transformed into spectral domain by  $Ux$  where  $\mathcal{L} = U^T \Lambda U$  (eigenvalue decomposition) and  $\mathcal{L}$  is normalized Laplacian matrix. If the convolution kernel is constrained as a function of  $\Lambda$ , a spectral convolution operator can be defined as

$$f(x; \theta) = U^T g(\Lambda; \theta) U x \quad (1)$$

Frequently, suppose that  $g(\Lambda; \theta)$  is diagonal and can be approximated by Chebyshev polynomials. If the linear approximation is utilized, the convolution can be defined as

$$f(x; \theta) = U^T (\theta_0 - \theta_1 \hat{\Lambda}) U x = (\theta_0 I - \theta_1 \hat{\mathcal{L}}) x \quad (2)$$

where  $\hat{\Lambda} = \frac{2}{\lambda_{max}} \Lambda - I$ . To reduce the amount of parameters to learn and simplify the graph convolutional network, suppose that  $\theta_0 = -\theta_1$ ,  $\lambda_{max} \approx 2$ . Accordingly, the above equation becomes  $f(x; \theta) = \theta_0 (I + D^{-\frac{1}{2}} \Lambda D^{-\frac{1}{2}}) x$ . Furthermore, we can renormalize the convolutional matrix as

$$\hat{\mathcal{L}} = \tilde{D}^{-\frac{1}{2}} (I + A) \tilde{D}^{-\frac{1}{2}} \quad (3)$$

where  $\tilde{D}_{ii} = \sum_{j=1}^n (I + A)_{ij}$ . Therefore, the processed signal can be rewritten as

$$f(x; \theta) = \theta_0 \hat{\mathcal{L}} x \quad (4)$$

If the graph signal is multiple-dimensional, i.e.,  $X \in \mathbb{R}^{n \times d}$ , and  $d'$  convolution kernels are applied, then we have

$$f(X; W) = \hat{\mathcal{L}} X W \quad (5)$$

where  $W \in \mathbb{R}^{d \times d'}$  is parameters to learn.

On the contrary, the mentioned convolution can be regarded as a spatial convolution operator since  $\hat{\mathcal{L}} X$  is equivalent to the weighted average of one node and its 1-neighbors. The intuitive explanation of general graph convolution network used in our model is shown in Figure 1.

#### 3.2. Graph Auto-Encoder

To apply GCN on clustering, graph auto-encoder (GAE) incorporates the traditional auto-encoder and GCN. Like

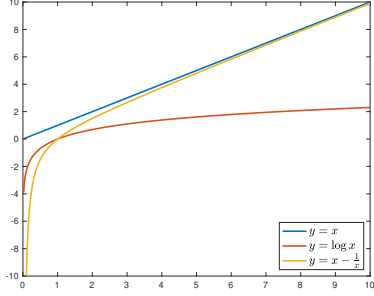


Figure 3. Illustration of mapping function  $\phi(x)$ . It is not hard to find that  $\phi(x)$  approximates  $y = x$  very fast with  $x$  increasing, and goes  $-\infty$  fast when  $x \rightarrow 0$ .

traditional auto-encoder, GAE consists of an encoder and a decoder.

**Encoder:** Encoder attempts to learn a latent representation  $Z$  of raw data via multiple graph convolution layers which have been introduced in previous subsection. In this paper, to keep simplicity, only simple GCN layers are employed. However, the encoder can be constituted by any valid layers such as attention, pooling, *etc.*

**Decoder:** Decoder intends to reconstruct the adjacency from the embedding. In network embedding, adjacency is usually given as prior and the graph is frequently unweighted. Therefore, the adjacency matrix  $A$  satisfies that  $A_{ij} = 1$  if the  $i$ -th point is connected with the  $j$ -th one;  $A_{ij} = 0$ , otherwise. Besides, similarity between two nodes is conventionally measured by inner-product. Specifically,  $z_i$  is analogous to  $z_j$  if  $z_i^T z_j$  is large enough. Therefore, the decoder is designed as  $\sigma(ZZ^T)$  where  $\sigma(\cdot)$  denotes the sigmoid function.

We further assume that all inner-products are non-negative, i.e.,  $ZZ^T \geq 0$ . This assumption is crucial for the embedded clustering model, joint clustering, which will be described in next subsection. The corresponding theoretical analysis will be shown in section 5. According to this, the activation function of the last encoding-layer should be non-negative (e.g., ReLU) so that  $Z \geq 0$ . However,  $\sigma(ZZ^T)$  will lie in  $[\frac{1}{2}, 1]$  which can not be regarded as probability. To address this issue, it is necessary to find a mapping function  $\phi(\cdot)$  which maps  $[0, +\infty)$  into  $(-\infty, +\infty)$  so that  $\sigma(\phi(ZZ^T))$  outputs valid probabilities. A natural choice is  $\log(x)$ . However,  $\log(x)$  is too insensitive to large values, which means that  $\sigma(\phi(x))$  will approach 1 slowly with  $x$  increasing. An ideal  $\phi(x)$  should approximate  $y = x$  when inputs are large enough. Motivated by this requirement, we design

$$\phi(x) = x - \frac{1}{x} \quad (6)$$

which is demonstrated in Figure 3. Hence, the decoder used

---

**Algorithm 1** Algorithm to optimize problem (10)

---

**Require:** Tradeoff parameters  $\alpha$  and  $\gamma$ , unnormalized Laplacian matrix  $L$  and normalized Laplacian matrix  $\mathcal{L}$ .

**repeat**

**repeat**

Calculate the gradients of Eq. (15) w.r.t.  $\{W_i\}_{i=1}^m$ :

$$\nabla J(\hat{A}, A) + \alpha \|Z - ZGG^T\|_F^2$$

Update GAE by gradient descent.

**until** convergence or exceeding maximum inner-iterations

Compute  $G$  by performing eigenvalue decomposition on  $Q$ .

**until** convergence or exceeding maximum outer-iterations

Perform k-means on row vectors of  $G$ .

**Ensure:** Clustering assignments, indicator matrix  $G$  and parameters  $\{W_i\}_{i=1}^m$ .

---

in our model is

$$\hat{A} = \sigma(\phi(ZZ^T)) \quad (7)$$

### 3.3. Proposed Model

As k-means partitions data via density information and spectral clustering takes local consistency into account, a clustering model incorporating both advantages is developed and is named as joint clustering, which is defined as

$$\min_{G^T G = I} \|X - FG^T\|_F^2 + \gamma \text{tr}(G^T LG) \quad (8)$$

where  $G$  is the relaxed indicator,  $L = D - A$  and  $\gamma$  is a tradeoff coefficient. The first term corresponds to k-means but with a continuous indicator  $G$ , while the second term is the Ratio Cut used spectral clustering.

Accordingly, the objective of GAE with Eq. (8) embedded is defined as

$$\min_{\hat{A}, Z, F, G^T G = I} J(\hat{A}, A) + \alpha (\|Z - FG^T\|_F^2 + \gamma \text{tr}(G^T LG)) \quad (9)$$

where  $J(\hat{A}, A)$  represents certain loss function that measures the reconstruction error between  $\hat{A}$  and  $A$ ,  $\alpha$  is the tradeoff coefficient and  $Z$  is extracted deep features. To avoid overfitting caused by GAE, a Lasso regularization is employed and the final objective function of EGAE-JOCAS is formulated as

$$\min_{\hat{A}, Z, F, G^T G = I} J(\hat{A}, A) + \alpha (\|Z - FG^T\|_F^2 + \gamma \text{tr}(G^T LG)) + \beta \sum_{i=1}^m \|W_i\|_{1,1} \quad (10)$$

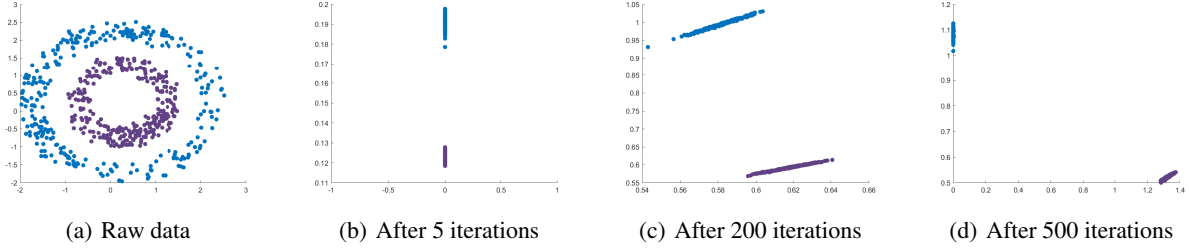


Figure 4. Illustration of EGAE-JOCAS on two-rings synthetic dataset

where  $W_i$  is parameters of the  $i$ -th layer,  $m$  is the amount of layers used in encoder and  $\|W\|_{1,1} = \sum_{i,j} |w_{ij}|$ . As the adjacency  $A$  is shared in both joint clustering and GAE, the spectral clustering term can be viewed as a regularization that utilizes prior structure information. Both of  $\gamma$  and  $\beta$  are pretty easy to choose and can be set as constants for all datasets for simplicity.

#### 4. Optimization

**Fix GAE and perform clustering:** As the GAE is fixed, the problem (10) is equivalent to

$$\min_{F, G^T G = I} \|Z - FG^T\|_F^2 + \gamma \text{tr}(G^T LG) \quad (11)$$

Since there is no constraint on  $F$ , we can take the derivative w.r.t.  $F$ ,

$$\begin{aligned} \frac{\partial \mathcal{J}}{\partial F} &= \frac{\partial \|Z - FG^T\|_F^2}{\partial F} \\ &= \frac{\partial \text{tr}((Z - FG^T)(Z^T - GF^T))}{\partial F} \\ &= -2ZG + 2F = 0 \end{aligned} \quad (12)$$

which means that

$$F = ZG \quad (13)$$

Substitute Eq. (13) into Eq. (11), and we have

$$\begin{aligned} &\min_{G^T G = I} \text{tr}(Z^T Z) - \text{tr}(G^T Z^T ZG) + \gamma \text{tr}(G^T LG) \\ &\iff \min_{G^T G = I} \text{tr}(G^T QG) \end{aligned} \quad (14)$$

where  $Q = \gamma L - Z^T Z$ .

Hence, the indicator matrix  $G$  can be computed by performing eigenvalue decomposition of  $Q$ . In other words, the optimal  $G$  consists of the leading  $c$  eigenvectors of  $Q$ .

**Update GAE with  $G$  and  $F$  fixed:** When clustering related variables are fixed as constants, the objective function is equivalent to

$$\min_{Z, \hat{A}} J(\hat{A}, A) + \alpha \|Z - ZGG^T\|_F^2 \quad (15)$$

which can be optimized by the standard gradient descent.

The procedure to solve problem (10) is summarized as Algorithm 1. The optimization can be viewed as optimizing GAE by gradient descent and solving the joint clustering via a close-form solution collaboratively. Hence, Algorithm 1 can be regarded as a modified coordinate descent algorithm.

#### 5. Motivation and Analysis

In this section, we will demonstrate the rationality of joint learning of GAE and the joint clustering from both intuitive aspect and theoretical aspect.

##### 5.1. Intuitive Illustration

To understand the motivation of EGAE-JOCAS, we give a visual interpretation via experiments on toy dataset. Roughly speaking, GAE, used in our model, can map data into a non-linear subspace which measures similarity via inner-products. Figure 4 illustrates the effect of EGAE-JOCAS built on orthogonality on 2-rings data. In the experiment, links among points of the same cluster are set with probability 0.9. From the figure, we realize that with the number of iterations increasing, 1) samples that connect with each other become more cohesive; 2) samples of different clusters go as orthogonal as possible. In other words, we can obtain orthogonal projected-points when the prior adjacency contains sufficient information.

In next subsection, we will prove that the relaxed k-means obtains optimal partition on orthogonal data and thus, it is vital to employ relaxed k-means as a part of embedded clustering model.

##### 5.2. Theoretical Analysis

When the embedding  $Z$  is fixed, the relaxed k-means is equivalent to

$$\max_{G^T G = I} \text{tr}(G^T Z^T ZG) \quad (16)$$

If the similarity is measured by inner-product which is non-negative, then  $Z^T Z$  can be regarded as similarity  $A$  among data points. It is pretty natural to integrate graph auto-



encoder and spectral relaxed k-means, as EGAE-JOCAS attempts to project raw data into a latent feature space which measures similarity among data points via inner-product. The following lemma and theorem shows us the spectral relaxed k-means can be applied on this type data.

**Lemma 1.**<sup>1</sup> For any positive and symmetric matrix  $K$ , the most principle component  $\alpha$  satisfies that all elements are not zero and have the same sign. More formally,

$$\forall i, j, \text{sign}(\alpha_i) = \text{sign}(\alpha_j) \quad (17)$$

**Theorem 1.** Provided that inner-products between any two data points are non-negative and two samples are orthogonal to each other if and only if they belong to different clusters, the spectral relaxed k-means can give an ideal partition.

*Proof.* If samples from different clusters are orthogonal and inner-products of samples from the same cluster are positive, then we have

$$A = ZZ^T = \begin{bmatrix} A^{(1)} & & & \\ & A^{(2)} & & \\ & & \ddots & \\ & & & A^{(c)} \end{bmatrix} \quad (18)$$

where  $A^{(i)} = Z_i^T Z_i$  and  $Z_i \in \mathbb{R}^{d \times n_i}$  consists of samples from the  $i$ -th cluster. According to our assumption, we have  $A^{(i)} > 0$ . With the help of Lemma 2, there exists  $\alpha_i$  which satisfies that

$$\begin{cases} \alpha_i > 0 \\ A^{(i)} \alpha_i = \lambda_{\max}^{(i)} \alpha_i \end{cases} \quad (19)$$

Furthermore,

$$A \begin{bmatrix} 0 \\ \alpha_i \\ 0 \end{bmatrix} = \lambda_{\max}^{(i)} \begin{bmatrix} 0 \\ \alpha_i \\ 0 \end{bmatrix} \quad (20)$$

Therefore, a valid relaxed  $G_0$  can be given as

$$G_0 = \text{diag}\left(\frac{\alpha_1}{\|\alpha_1\|_2}, \frac{\alpha_2}{\|\alpha_2\|_2}, \dots, \frac{\alpha_c}{\|\alpha_c\|_2}\right) \quad (21)$$

However, given a orthogonal matrix  $R$ , any  $G$  which satisfies  $G = G_0 R$  is a valid solution. If we normalize rows of  $G$  as  $\hat{G}$ , then we have

$$\hat{G} = [\pm \mathbf{1}_{n_1} \mathbf{r}^1; \pm \mathbf{1}_{n_2} \mathbf{r}^2; \dots; \pm \mathbf{1}_{n_c} \mathbf{r}^c] \quad (22)$$

Accordingly, it will obtain ideal partition if the k-means is performed on rows of  $\hat{G}$ .  $\square$

The following theorem will show the connection between the relaxed k-means and normalized cut spectral clustering.

<sup>1</sup>Due to limitation of space, the proof is stated in supplementary material.

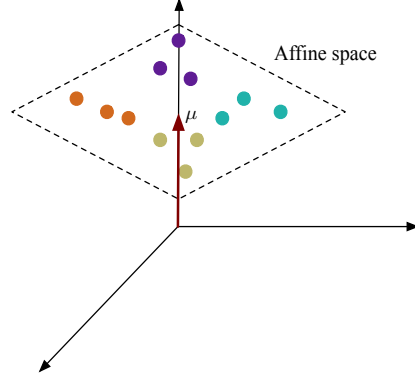


Figure 5. Illustration of Theorem 2

**Theorem 2.** Problem (16) is equivalent to spectral clustering with normalized cut if and only if the mean vector  $\mu$  is perpendicular to the centralized data, or equivalently,  $\mu$  is perpendicular to the affine space that all data points lie in.

*Proof.* The objective function of normalized cut spectral clustering is given as

$$\begin{aligned} & \min_{G^T G = I} \text{tr}(G^T \mathcal{L} G) \\ & \Rightarrow \min_{G^T G = I} \text{tr}(I - G^T D^{-\frac{1}{2}} A D^{-\frac{1}{2}} G) \\ & \Rightarrow \max_{G^T G = I} \text{tr}(G^T D^{-\frac{1}{2}} A D^{-\frac{1}{2}} G) \end{aligned} \quad (23)$$

Note that  $D = \text{diag}(Z^T Z \mathbf{1}) = n \times \text{diag}(Z^T \mu)$ . Let  $H = I_n - \frac{1}{n} \mathbf{1}_n \mathbf{1}_n^T$  be a centralized matrix. Then the centralized data can be represented as  $\hat{Z} = ZH = Z - \mu \mathbf{1}_n^T$ .

On the one hand, if  $\mu$  is perpendicular to the centralized data, then we have

$$\hat{Z}^T \mu = Z^T \mu - \mathbf{1}_n \mu^T \mu = Z^T \mu - \|\mu\|_2^2 \mathbf{1}_n = 0 \quad (24)$$

which means

$$D = n \times \text{diag}(\|\mu\|_2^2 \mathbf{1}_n) = n \|\mu\|_2^2 I_n \quad (25)$$

Hence, problem (23) has the same solution with problem (16). On the other hand, if problem (16) is equivalent to problem (23),  $D = kI_n$ . Therefore, we have

$$H Z^T Z \mathbf{1}_n = H Z^T \cdot n \mu = 0 \quad (26)$$

Accordingly,  $\text{rank}(H^T Z) < d$  which means that data points lie in an affine space, and the centralized data is perpendicular to  $\mu$ .

Hence, the theorem is proved.  $\square$

Figure 5 gives an intuitive illustration of Theorem 2 when samples have 3 dimensions and lie in a 2-dimension affine space.

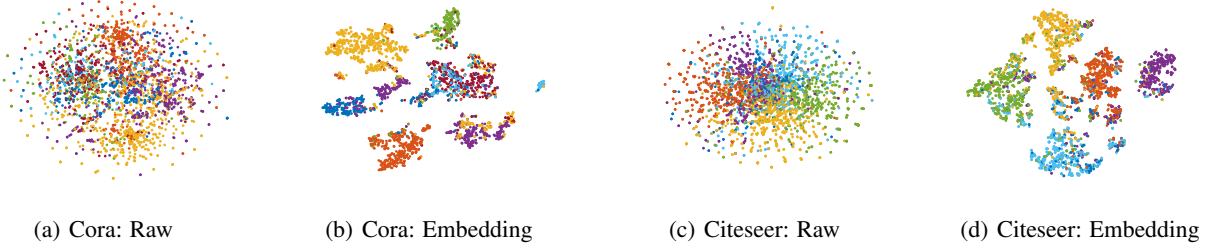


Figure 6. t-SNE visualization of EGAE-JOCAS

Although the ideal condition seems to be too rigorous, EGAE-JOCAS has the ability to project points into a non-linear feature space that data points assigned to different clusters are orthogonal (uncorrelated) to each other.

## 6. Experiment

We state crucial details of experiments and clustering results of EGAE-JOCAS. The visualization is shown in Figure 6. In particular, we extend experiments into traditional datasets besides two graph type datasets.

### 6.1. Benchmark Datasets

To verify the effectiveness of EGAE-JOCAS, experiments are conducted on not only datasets with prior adjacency but also normal datasets that need to construct adjacency at first.

**Cora** and **Citeseer** consist of adjacency and content. Each node represents a publication and link denotes a citation between two papers. Content features correspond to a word vector. **YALE** (Georghiades et al., 2001) and **UMIST** (Hou et al., 2013) are traditional human faces datasets, which have no adjacency. The information of datasets is summarized in Table 1.

### 6.2. Baseline Methods

Totally ten algorithms are compared in the experiments: **K-means**, Spectral Clustering (SC), **Graph Encoder** (Tian et al., 2014b), **Deep Walk** (Perozzi et al., 2014), **DNGR** (Cao et al., 2016), **GAE (VGAE)** (Kipf & Welling, 2016), **ARGE (ARVGE)** (Pan et al., 2018), **KKM** (Dhillon

Dataset	# Nodes	# Links	# Features	# Classes
Cora	2,708	5,429	1,433	7
Citeseer	3,312	4,732	3,703	6
YALE	165	—	1,024	15
UMIST	575	—	1,024	20

Table 1. Concrete Information of Datasets

Methods	ACC	NMI	Precision
Graph Encoder	0.325	0.109	0.182
DeepWalk	0.484	0.327	0.361
DNGR	0.419	0.318	0.266
GAE	0.596	0.429	0.596
VGAE	0.609	0.436	0.609
ARGE	0.640	0.449	0.646
ARVGE	0.638	0.450	0.624
<b>Ours with <math>\alpha = 0</math></b>	0.563	0.431	0.563
<b>Ours with <math>\beta = 0</math></b>	0.609	0.433	0.609
<b>EGAE-JOCAS</b>	<b>0.686</b>	<b>0.536</b>	<b>0.672</b>

Table 2. Clustering Results on Cora

Methods	ACC	NMI	Precision
Graph Encoder	0.225	0.033	0.179
Deep Walk	0.337	0.088	0.248
DNGR	0.326	0.180	0.200
GAE	0.408	0.176	0.418
VGAE	0.344	0.156	0.349
ARGE	0.573	0.350	0.573
ARVGE	0.544	0.261	0.549
<b>Ours with <math>\alpha = 0</math></b>	0.453	0.221	0.454
<b>Ours with <math>\beta = 0</math></b>	0.524	0.318	0.524
<b>EGAE-JOCAS</b>	<b>0.674</b>	<b>0.405</b>	<b>0.626</b>

Table 3. Clustering Results on Citeseer

et al., 2004), **Auto-Encoder** (Hinton & Salakhutdinov, 2006), **DEC** (Xie et al., 2016). To test the effectiveness of different parts of EGAE-JOCAS, we conduct ablation experiments with  $\alpha = 0$  and  $\beta = 0$ .

For Cora and Citeseer, only models designed for network embedding are used as competitors while for YALE and UMIST, several representative methods are compared.

### 6.3. Experimental Settings

In our experiments, the encoder is a two-layer GCN. Activation functions of the first layer and the second layer are

Methods	YALE		UMIST	
	ACC	NMI	ACC	NMI
K-Means	0.384	0.482	0.419	<u>0.648</u>
SC	0.296	0.348	0.290	0.308
KKM	0.390	0.467	<u>0.429</u>	0.639
Auto-Encoder	0.402	0.469	0.426	0.638
DEC	<u>0.423</u>	<u>0.487</u>	0.365	0.570
GAE	0.315	0.357	0.388	0.522
<b>EGAE-JOCAS</b>	<b>0.453</b>	<b>0.524</b>	<b>0.475</b>	<b>0.690</b>

Table 4. Clustering Results on YALE

linear function and ReLU, respectively. Although  $\beta$  and  $\gamma$  are hyper-parameters to tune manually, it is pretty easy to set them. In our experiments, we set  $\beta = 10^{-3}$  and  $\gamma = 10^{-3}$  empirically. Hence, there is only one tradeoff coefficient,  $\alpha$ , to tune. We search  $\alpha$  in the range of  $\{10^{-3}, 10^{-2}, 10^{-1}, 10^0, 10^1, 10^2, 10^3\}$ . The maximum inner-iteration is set as 10 and the maximum outer-iteration is set as 50. Besides, the learning rate is set as  $10^{-3}$ .

For Cora and Citeseer, the encoder is composed of 32-neurons hidden layer and 16-neurons embedding layer. As the adjacency is unweighted and discrete,  $J(\cdot, \cdot)$  is the cross entropy loss function. For YALE and UMIST, the encoder has a 200-neuron hidden layer and a 50-neuron embedding layer. As no adjacency is provided as priori, the following formulation is employed to construct adjacency

$$\bar{A}_{ij} = \frac{K(z_i, z_j)}{\sum_{k \in \mathcal{N}_i} K(z_i, z_k)}, \forall z_j \in \mathcal{N}_i \quad (27)$$

where  $K(\cdot, \cdot) = \exp(-\frac{\|z_i - z_j\|_2^2}{\sigma})$  and  $\mathcal{N}_i$  is 5-nearest neighbors of the  $i$ -th sample. Otherwise,  $\bar{A}_{ij} = 0$ . Then  $A$  is computed by  $A = (\bar{A} + \bar{A}^T)/2$ . Mean square error (MSE) is chosen as  $J(\cdot, \cdot)$  since constructed adjacency is weighted and continuous. All methods are performed 10 times and the means are reported. More details is stated in supplementary.

#### 6.4. Experimental Results

**Graph type datasets:** Clustering results of Cora and Citeseer are reported in Table 2 and 3 respectively. On both of Cora and Citeseer, GAE and its extensions outperform other network embedding models. Specifically speaking, GAE increases ACC more than 10 percent compared with Deep Walk. Similar with traditional auto-encoder, GAE suffers from overfitting. ARGE and ARVG absorb adversarial learning into GAE to address this issue and thus promote the performance. In particular, EGAE-JOCAS obtains remarkable results on all metrics with the same structure of encoder. Compared with GAE, EGAE-JOCAS embeds joint clustering into GAE so that the extracted deep features are more appropriate for clustering.

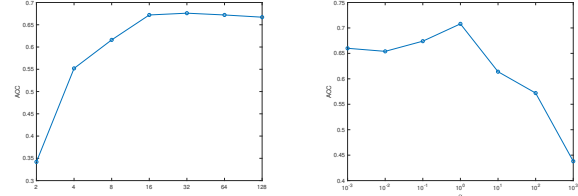
(a) Dimension ( $\alpha = 10^{-3}$ ) (b)  $\alpha$  (dimension is set as 16)

Figure 7. Impact of embedding dimension and  $\alpha$  on Cora. The left one shows the impact of embedding dimension and the right one shows the impact of  $\alpha$ .

**Traditional datasets:** Clustering results of YALE and UMIST are reported in Table 4. Since GAE suffers from overfitting, it works worse than Auto-Encoder. On the contrary, EGAE-JOCAS alleviates overfitting by adopting the designed joint clustering. Besides, it utilizes the structure information of data so that it achieves better results.

#### 6.5. Parameter Study

In our experiments, we focus on the impact of embedding dimension and  $\alpha$ . Embedding dimension varies in  $\{2, 4, 8, 16, 32, 64, 128\}$  and  $\alpha$  varies in  $\{10^{-3}, 10^{-2}, 10^{-1}, 10^0, 10^1, 10^2, 10^3\}$ . Figure 7 demonstrates different performance with different settings on Cora. From the left one, we find that ACC keeps stable when dimension arrives 16. Although nodes in Cora belong to only 7 classes and the embedding dimension just needs to be 7 in theory, too small embedding dimension is hard to learn. Accordingly, the embedding layer is set as a 16-neuron graph convolution layer for Cora and Citeseer. From the right one, ACC keeps high when  $\alpha$  is not more than 1. Too large  $\alpha$  may lead to generate terrible embedding.

### 7. Conclusion

In this paper, we propose a novel GAE based clustering model, namely Embedding Graph Auto-Encoder with JOint Clustering via Adjacency Sharing (EGAE-JOCAS). On the one hand, to design a clustering model that is suitable for network embedding, we design a novel clustering model, joint clustering, which integrates advantages of k-means and spectral clustering. The joint clustering is embedded into GAE to generate better representations. The optimization process is to optimize GAE and perform clustering simultaneously. On the other hand, a modified GAE is developed for joint clustering. Analysis stated in section 5 demonstrate the rationality of EGAE-JOCAS. Although the precondition seems too strict to achieve, the non-linear feature space generated by GAE has many similar characteristics with the ideal space. Extensive experiments prove the superiority on both of graph type datasets and traditional datasets.



## References

- Bojchevski, A., Shchur, O., Zügner, D., and Günnemann, S. Netgan: Generating graphs via random walks. *arXiv preprint arXiv:1803.00816*, 2018.
- Bruna, J., Zaremba, W., Szlam, A., and LeCun, Y. Spectral networks and locally connected networks on graphs. *arXiv preprint arXiv:1312.6203*, 2013.
- Cao, S., Lu, W., and Xu, Q. Deep neural networks for learning graph representations. In *Thirtieth AAAI Conference on Artificial Intelligence*, 2016.
- Dhillon, I., Guan, Y., and Kulis, B. Kernel k-means: spectral clustering and normalized cuts. In *Proc. ACM SIGKDD Int. Conf. Knowl. Dis. Data Mining*, pp. 551–556, 2004.
- Dunn, J. A fuzzy relative of the isodata process and its use in detecting compact well-separated clusters. 3(3):32–57, 1973.
- Ester, M., Kriegel, H., Sander, J., and Xu, X. Density-based algorithm for discovering clusters in large spatial databases with noise. In *KDD*, pp. 226–231, 1996.
- Georgiades, A., Belhumeur, P., and Kriegman, D. From few to many: Illumination cone models for face recognition under variable lighting and pose. *IEEE Transactions on Pattern Analysis & Machine Intelligence*, (6):643–660, 2001.
- Hinton, G. E. and Salakhutdinov, R. Reducing the dimensionality of data with neural networks. *Science*, 313 (5786):504–507, 2006.
- Hou, C., Nie, F., Li, X., Yi, D., and Wu, Y. Joint embedding learning and sparse regression: A framework for unsupervised feature selection. *IEEE Transactions on Cybernetics*, 44(6):793–804, 2013.
- Kipf, T. N. and Welling, M. Variational graph auto-encoders. *arXiv preprint arXiv:1611.07308*, 2016.
- Kipf, T. N. and Welling, M. Semi-supervised classification with graph convolutional networks. *Proc. of ICLR*, 2017.
- Kushnir, D., Galun, M., and Brandt, A. Fast multiscale clustering and manifold identification. *Pattern Recognition*, 39(10):1876–1891, 2006.
- Liu, L., Xu, L., Wangy, Z., and Chen, E. Community detection based on structure and content: A content propagation perspective. In *2015 IEEE International Conference on Data Mining*, pp. 271–280. IEEE, 2015.
- Micheli, A. Neural network for graphs: A contextual constructive approach. *IEEE Transactions on Neural Networks*, 20(3):498–511, 2009.
- Ng, A., Jordan, M., and Weiss, Y. On spectral clustering: Analysis and an algorithm. In *Advances in neural information processing systems*, pp. 849–856, 2002.
- Nie, F., Wang, X., and Huang, H. Clustering and projected clustering with adaptive neighbors. In *Proc. ACM SIGKDD Int. Conf. Knowl. Discovery Data Mining*, pp. 977–986, 2014.
- Niepert, M., Ahmed, M., and Kutzkov, K. Learning convolutional neural networks for graphs. In *International conference on machine learning*, pp. 2014–2023, 2016.
- Pan, S., Hu, R., Long, G., Jiang, J., Yao, L., and Zhang, C. Adversarially regularized graph autoencoder for graph embedding. In *IJCAI*, pp. 2609–2615, 2018.
- Peng, X., Feng, J., Xiao, S., Yau, W., Zhou, T., and Yang, S. Structured autoencoders for subspace clustering. *IEEE Transactions on Image Processing*, 27(10):5076–5086, 2018.
- Perozzi, B., Al-Rfou, R., and Skiena, S. Deepwalk: Online learning of social representations. In *Proceedings of the 20th ACM SIGKDD international conference on Knowledge discovery and data mining*, pp. 701–710. ACM, 2014.
- Scarselli, F., Gori, M., Tsoi, A. C., Hagenbuchner, M., and Monfardini, G. The graph neural network model. *IEEE Transactions on Neural Networks*, 20(1):61–80, 2008.
- Shaham, U., Stanton, K., Li, H., Basri, R., Nadler, B., and Kluger, Y. Spectralnet: Spectral clustering using deep neural networks. In *International Conference on Learning Representations*, 2018.
- Shi, J. and Malik, J. Normalized cuts and image segmentation. *IEEE Trans. Pattern Anal. Mach. Intell.*, 22(8): 888–905, 2000.
- Shuman, D. I., Narang, S. K., Frossard, P., Ortega, A., and Vandergheynst, P. The emerging field of signal processing on graphs: Extending high-dimensional data analysis to networks and other irregular domains. *IEEE Signal Processing Magazine*, 30(3):83–98, 2013.
- Tian, F., Gao, B., Cui, Q., Chen, E., and Liu, T. Learning deep representations for graph clustering. In *Twenty-Eighth AAAI Conference on Artificial Intelligence*, pp. 1293–1299, 2014a.
- Tian, F., Gao, B., Cui, Q., Chen, E., and Liu, T.-Y. Learning deep representations for graph clustering. In *Twenty-Eighth AAAI Conference on Artificial Intelligence*, pp. 1293–1299, 2014b.

Veličković, P., Cucurull, G., Casanova, A., Romero, A., Lio, P., and Bengio, Y. Graph attention networks. *arXiv preprint arXiv:1710.10903*, 2017.

Wang, H., Wang, J., Wang, J., Zhao, M., Zhang, W., Zhang, F., Xie, X., and Guo, M. Graphgan: Graph representation learning with generative adversarial nets. In *Thirty-Second AAAI Conference on Artificial Intelligence*, pp. 2508–2515, 2018.

Wang, X., Cui, P., Wang, J., Pei, J., Zhu, W., and Yang, S. Community preserving network embedding. In *Thirty-First AAAI Conference on Artificial Intelligence*, pp. 203–209, 2017.

Wu, Z., Pan, S., Chen, F., Long, G., Zhang, C., and Yu, P. S. A comprehensive survey on graph neural networks. *arXiv preprint arXiv:1901.00596*, 2019.

Xie, J., Girshick, R., and Farhadi, A. Unsupervised deep embedding for clustering analysis. In *International Conference on Machine Learning*, pp. 478–487, 2016.

## A. Proof of Lemma 1

**Lemma 2.** For any positive and symmetric matrix  $K$ , the most principle component  $\alpha$  satisfies that all elements are not zero and have the same sign. More formally,

$$\forall i, j, \text{sign}(\alpha_i) = \text{sign}(\alpha_j) \quad (28)$$

*Proof.* According to the definition, we have

$$\begin{cases} \alpha = \arg \max_{\mathbf{x}} \frac{\mathbf{x}^T K \mathbf{x}}{\mathbf{x}^T \mathbf{x}} \\ \lambda_{max} = \max_{\mathbf{x}} \frac{\mathbf{x}^T K \mathbf{x}}{\mathbf{x}^T \mathbf{x}} \end{cases} \quad (29)$$

Suppose that  $\exists i, j, \text{sign}(\alpha_i) \neq \text{sign}(\alpha_j)$ . We can construct  $\hat{\alpha} = |\alpha|$ . Note that

$$\mathbf{x}^T K \mathbf{x} = \sum_{i,j} k_{ij} x_i x_j \quad (30)$$

As  $K > 0$ , we have

$$\hat{\alpha}^T K \hat{\alpha} = \sum_{i,j} k_{ij} |\alpha_i \alpha_j| > \sum_{i,j} k_{ij} \alpha_i \alpha_j = \alpha^T K \alpha \quad (31)$$

Moreover,  $\hat{\alpha}^T \hat{\alpha} = \alpha^T \alpha$ . Hence, we have

$$\frac{\hat{\alpha}^T K \hat{\alpha}}{\hat{\alpha}^T \hat{\alpha}} = \frac{\hat{\alpha}^T K \hat{\alpha}}{\alpha^T \alpha} > \frac{\alpha^T K \alpha}{\alpha^T \alpha} \quad (32)$$

which leads to a contradiction. Therefore,  $\alpha \geq 0$  or  $\alpha \leq 0$ .

Due to  $K > 0$ ,  $\text{tr}(K) = \sum_i k_{ii} > 0$ . Clearly, we have  $\lambda_{max} > 0$ . If  $\alpha_k = 0$ , then we have

$$\beta = K \alpha = \sum_{i \neq k} k_{ik} \alpha_i \quad (33)$$

Note that

$$K \alpha = \lambda_{max} \alpha \quad (34)$$

It is not hard to verify that  $\beta_k = \lambda_{max} \alpha_k$  if and only if  $\alpha = 0$ , which leads to a contradiction. Therefore,  $\alpha < 0$  or  $\alpha > 0$ .

Hence, the lemma is proved.  $\square$

## B. Time Complexity

Let  $d_0$  be the dimension of raw features and  $d_i$  be dimension of the  $i$ -th layer’s output. Since each propagation needs all samples in dataset, every update step of GAE needs  $O(n^2 \sum_{i=0}^k (d_i d_{i+1}))$  time. The optimization of clustering model needs  $O(n^2 c)$  to perform eigenvalue decomposition. It should be pointed out that if  $\gamma = 0$ , then we can speed it up by singular value decomposition (SVD) which only needs  $O(nd_k c)$  time. Let  $l_i$  be the inner-iterations and  $l_o$  be the outer-iterations, and the time complexity of EGAE-JOCAS is  $O(l_o(l_i n^2 \sum_{i=0}^k (d_i d_{i+1}) + n^2 c))$ . Apparently, the embedded clustering model does not increase the complexity of GAE as  $c$  is usually small compared with  $d_i$ .

Datasets	$\alpha$	$\gamma$	$\beta$	I-Iter	O-Iter	P-Iter	Learning Rate	Struct	Loss
Cora	0.001	0.01	0.001	10	30	10	0.001	32-16	Cross-Entropy
Citeseer	0.001	0.01	0.001	10	30	10	0.001	32-16	Cross-Entropy
YALE	1000	0.01	0.001	10	30	100	0.001	500-20	MSE
UMIST	100	0.01	0.001	10	20	100	0.001	500-20	MSE

Table 5. Concrete settings of EGAE-JOCAS for four different datasets

### C. More Details of Experiments

In this section, we will give crucial details of our experiments. Besides, the exact values of hyper parameters are provided.

In our experiments, the maximum iteration to optimize EGAE-t is represented as **Outer-Iteration (O-Iter)**, and the maximum iteration to optimize GAE in each outer-step is represented as **Inner-Iteration (I-Iter)**. To initialize GAE, we first train GAE without joint clustering embedded and iteration to optimize it is denoted by **Pre-Iteration (P-Iter)**. **Struct** denotes the topological structure of encoder used in EGAE-JOCAS. **Loss** represents the employed loss function  $J(\cdot, \cdot)$ . The concrete settings are summarized in Table 5.

To apply EGAE-JOCAS on traditional datasets (YALE and UMIST), the adjacency matrix need to be constructed by

$$\bar{A}_{ij} = \frac{K(\mathbf{z}_i, \mathbf{z}_j)}{\sum_{k \in \mathcal{N}_i} K(\mathbf{z}_i, \mathbf{z}_k)}, \forall \mathbf{z}_j \in \mathcal{N}_i \quad (35)$$

where

$$K(\mathbf{z}_i, \mathbf{z}_j) = \exp\left(-\frac{\|\mathbf{z}_i - \mathbf{z}_j\|_2^2}{\sigma}\right) \quad (36)$$

and  $\mathcal{N}_i$  denotes  $c$ -nearest neighbors. In this paper, we set  $c = 5$  for YALE and UMIST. Moreover, the bandwidth coefficient  $\sigma$  is set as

$$\sigma = \frac{1}{n^2} \sum_{i,j=1}^n \|\mathbf{z}_i - \mathbf{z}_j\|_2^2 \quad (37)$$

All experiments are run under tensorflow-1.14.0-cpu on Windows 10 with 8 i7 cores and 16GB main memory.